Int. J. Heat Mass Transfer. Vol. 10, pp. 1225–1232. Pergamon Press Ltd. 1967. Printed in Great Britain

HEMISPHERICAL REFLECTANCE OF METAL SURFACES AS A FUNCTION OF WAVELENGTH AND SURFACE ROUGHNESS

R. C. BIRKEBAK*, J. P. DAWSON†, B. A. McCULLOUGH‡ and B. E. WOOD‡

(*Received* 6 *April* 1966 *and in revised form* 30 *March* 1967)

Abstract—Measurements of the hemispherical reflectance of metallic surfaces with controlled uniform surface roughness were made using a sulfur infrared integrating sphere and a Beckman DK-2A spectrometer. The surfaces studied were ground glass and nickel coated with films of aluminum, gold, platinum, and nickel. The data indicate that beyond a ratio of surface roughness to incident wavelength, $\sigma_0/\lambda \cong 1$, the normalized data for aluminum, gold, platinum may be represented by a single curve. This was true for both uniform unidirectional and isotropic roughnesses, although the nickel data deviate from this curve. The causes for this deviation are believed to be associated with surface stresses caused by changes in the crystalline structure and are discussed in this paper.

NOMENCLATURE

a, parameter connected to the RMS slope M of the surface contour through the relation $(\sqrt{2})\,[\sigma/M]$.

Greek symbols

- θ, angle between reflected radiation and surface normal;
- λ, wavelength;
- ρ, reflectance;
- σ, root-mean-square surface roughness;
- φ, angle of reflected radiation measured in plane of reflecting surface;
- ψ, angle between incident radiation and surface normal;
- ω, solid angle.

Subscripts

- ah, angular-hemispherical;
- ba, biangular;
- ha, hemispherical-angular;
- i, incident;
- m, mechanical;
- o, optical;
- p, smooth polished surface;
- r, reflected;
- s, specular;
- V, viewing direction.

INTRODUCTION

RADIATIVE reflectance of a material has been shown to be a function of surface roughness [1, 2] and surface contaminants. Therefore, the relationship between these factors must be known for accurate heat balance studies.

Until recently, a theory relating uniform surface roughness and reflectance has been lacking. In 1954 Davies proposed a mathematical model which would predict the scattering of μ-waves from disturbed water surfaces. In 1961 Bennett and Porteus applied Davies' theory to reflected light from metal surfaces of specific roughnesses and verified its application in the infrared region for the case of near normal incidence and specular reflectance.

Several experimental investigations of interest

* University of Kentucky.
† Manned Spacecraft Center, NASA, Houston, Texas.
‡ ARO, Inc., Aerospace Environmental Facility, Arnold Engineering Development Center, Arnold Air Force Station, Tennessee.

to this paper on the relationship between the roughness of surfaces and the specular or diffuse reflectance have been reported [2–4]. Radiation in the visible and near infrared region was used, and the reflectance was measured for various angles of incidence. In the visible regime, the surface irregularities are comparable in magnitude to the radiation wavelength, and the specular reflectance is also a function of the r.m.s. surface roughness and slope [1, 5]. In the infrared, the specular reflectance is primarily a function of the RMS surface roughness. Using the Davies–Bennett theory, the optical surface roughness may be calculated from infrared reflectance data, and the RMS slope may be obtained from visible reflectance measurements.

In a recent paper by Birkebak and Eckert [2], biangular, specular, and hemispherical–angular reflectance measurements of roughened aluminum and nickel surfaces were discussed in terms of the surface roughness, σ_o, and wavelength, λ. In their conclusions, the authors recommended additional studies be made of the effects of surface material on the hemispherical–angular reflectances. This report expands the surface material effects on the hemispherical–angular reflectance in terms of new measurements and additional calculations. The discussion centers around the wavelength range where the hemispherical–angular reflectance is essentially constant and independent of the optical surface roughness ratio, σ_o/λ. The test surfaces studied were films of aluminum, gold, platinum, and nickel applied on roughened substrates of glass and pure nickel.

TEST SURFACES

The test surfaces were prepared by a standard optical grinding technique using aluminum oxide grinding compounds of various grit sizes. In this technique, the sample is free to rotate around its own center while moving back and forth across the rotating grinding wheel.

Ground glass was chosen as the substrate material because it obtains a very irregular surface in the grinding process. All ground surfaces were coated simultaneously with an evaporated metal film to a thickness of approximately 8×10^{-6} in. In the following figures, the various samples are identified by their surfaces roughness, σ_m, which was measured mechanically with a Cleveland Model BK6101 roughness indicator. The RMS mechanical and optical surface roughnesses for metal-coated glass samples are given in Table 1 of [2].

The nickel surfaces were prepared using the same techniques described for the ground glass surfaces. The mechanical and optical surface roughnesses are given in Table 2 of [2].

A metal-coated polished glass sample and a polished nickel sample were used as reference surfaces in their respective measurements [2]. The surface irregularities of these samples were an order of magnitude smaller than those of the smoothest roughened sample.

MEASUREMENT TECHNIQUES AND PROCEDURES

The angular–hemispherical technique (*ah*) was employed in the reflectance measurements in the visible and near infrared region. This technique is shown in Fig. 1(a). The incident radiation is contained in the solid angle $\Delta\omega_i$, and the radiation, which is reflected hemispherically, is measured. The hemispherical–angular technique (*ha*) was used in the infrared measurements. In this technique (Fig. 1b), the test surface is irradiated hemispherically, and the energy reflected in a particular solid angle $\Delta\omega_r$ is measured. A discussion by Torrance and Sparrow appended to [2] showed that the two techniques are equivalent if the angle ψ_i for ρ_{ah} is equal to the angle θ_V for ρ_{ha}. The solid angles $\Delta\omega_i$ and $\Delta\omega_r$, used in this study, were approximately equal, and ψ_i = approximately 15° and θ_V = 10°. This difference is ψ_i and θ_V was caused by the different geometries of the two systems; however, no difference was noted in the data in the overlap region.

The system used to measure the hemispherical–angular reflectance was identical to that described in [2]. It consisted of an integrating sphere, a radiation source, a focusing mirror, and a monochromator. The sample was uniformly radiated by the source and multiple reflections from the sulfur interior of the integrating sphere. The energy reflected at an angle of $\theta_V = 10°$ from the normal was viewed by a mirror. This energy was focused on the entrance slit of the monochromator and the intensity measured by the detector. The angular–hemispherical system employed was a standard Beckman DK-2A spectrophotometer with a magnesium oxide-coated integrating sphere attachment. The angle of incident energy was approximately 15° from the normal.

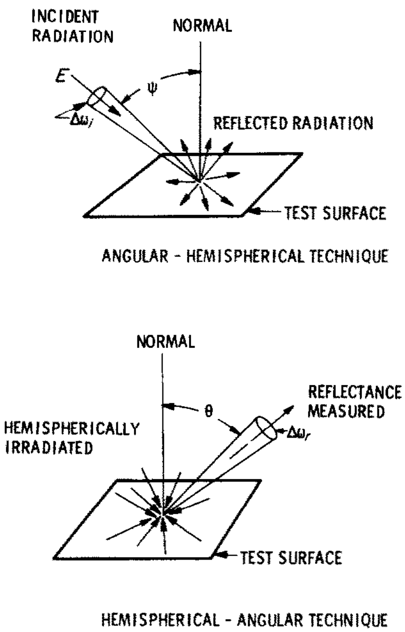

FIG. 1. Reflectance definition and coordinates.

Using either technique, the test surface was placed in the integrating sphere. The surface was irradiated, and the energy reflected was measured as a function of wavelength. The reflectance of each roughened surface was compared to the respective polished sample and to a standard sample. The standard samples used were magnesium oxide in the 0·35–2·7-μ range and flowers of sulfur from 1·5 to 15 μ.

RESULTS AND DISCUSSION

According to Birkebak and Eckert [2] in their discussion on the hemispherical–angular reflectance, ρ_{ha}, the theory of Davies [5] indicates the ρ_{ha} is independent of wavelength for $\lambda \leqslant \sigma_o$. The results [2] shown in Fig. 2 for the biangular reflectance normalized with respect to the specular ray reflectance indicate that over a

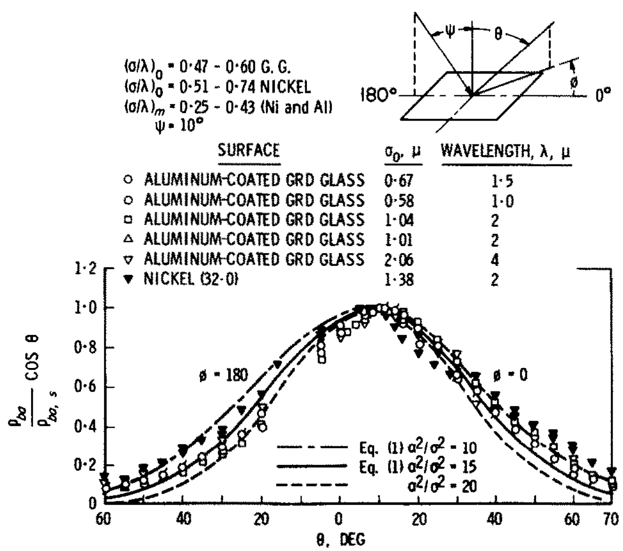

FIG. 2. Biangular reflectance correlations.

range of surface roughness from 0·6 to 2 μ and wavelength range from 1 to 4 μ that the results are independent of wavelength. The angular values of θ were limited to approximately two-thirds its total range because of lack of data for the majority of the surfaces beyond 70°.

The ratio of the hemispherical-angular reflectance of the rough surface to that of a polished sample of the same material plotted versus the optical roughness ratio, σ_0/λ, is shown in Figs. 3 and 4 for aluminum, gold, nickel, and platinum. The coated surfaces (Fig. 3) approach an asymptotic hemispherical-angular reflectance value about twice that of the nickel value (open symbols, Fig. 4). The variation of the hemispherical-angular reflectance with film material is the subject of the remaining section of this paper.

In order to evaluate this effect, the test surfaces studied in [2] (evaporated films of pure aluminum on ground glass and roughened nickel samples) were restudied. Using these test samples as substrate surfaces, evaporated films of gold, platinum, and nickel were deposited and the reflectances measured as a function of wavelength from 0·5 to 2 μ.

The data are presented as the ratio of the hemispherical-angular reflectance of a roughened surface to that of a perfectly smooth surface (σ_0 = 0·003 μ) of the same material, $\rho_{ha}/\rho_{ha,p}$ vs.

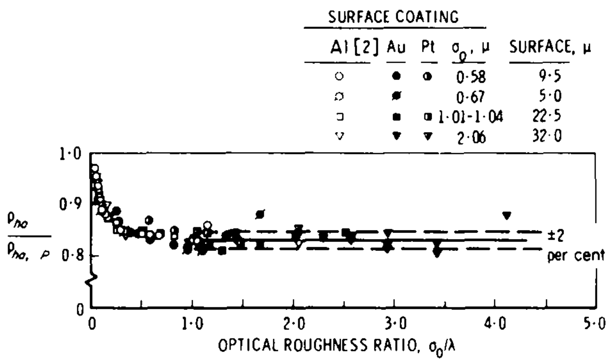

FIG. 3. Hemispherical-angular reflectance, ground glass substrate.

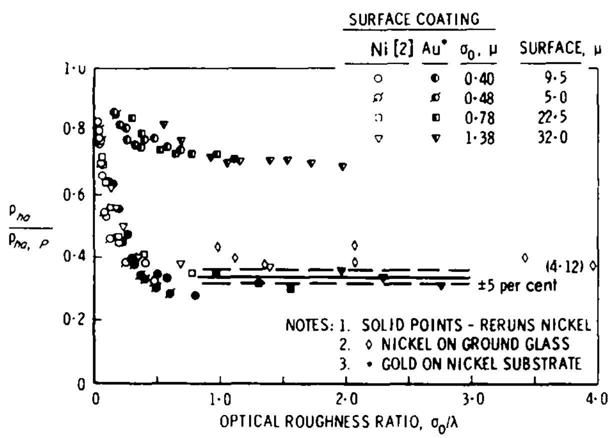

FIG. 4. Hemispherical-angular reflectance, nickel substrate.

the ratio of the optical RMS roughness to wavelength, σ_0/λ, where σ_0 was determined previously in [2].

Since the nickel surfaces had been exposed to excessive handling, they were restudied after having been cleaned. There was no indication that any major change had occurred in the roughness distribution at the wavelengths used. The results are shown in Fig. 4 (solid points) and satisfactory agreement is obtained where the two sets of data overlap.

between ground nickel, gold, platinum, or aluminum remains to be explained.

To resolve this peculiar behavior of nickel, sputtered films of pure nickel were applied to some of the ground glass samples. The data (Fig. 4) agree within experimental error with the results in [2] for pure nickel surfaces. Therefore, it must be concluded that the cause is primarily associated with the nickel surfaces [6].

Further examination of the results in [2] reveals that when the angular–hemispherical

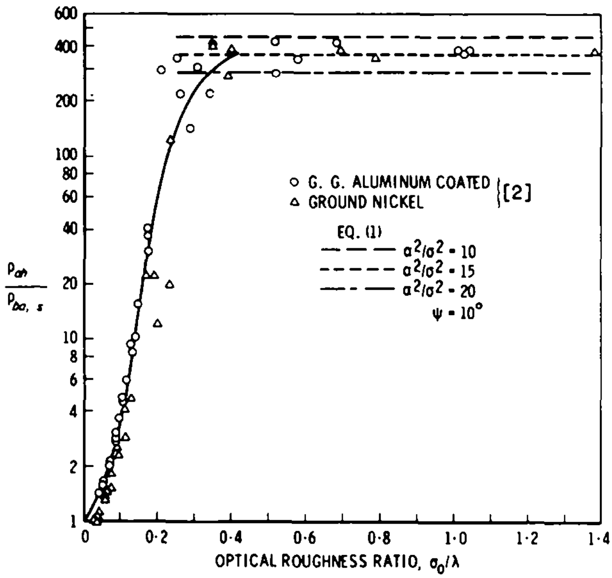

FIG. 5. Hemispherical–specular function vs. optical roughness ratio.

The hemispherical–angular reflectance results* of gold and platinum on ground glass agree within 2 per cent with those of aluminum (Fig. 3). The results for gold on a nickel substrate show a change in hemispherical–angular reflectance by a factor of 2 as compared to nickel and are in fair agreement with those of gold on ground glass. These results indicate that the surface materials of aluminum, gold and platinum do not affect the normalized hemispherical–angular reflectance. However, the discrepancy

* It was assumed that the optical roughness σ_0 is independent of the film.

reflectance is normalized with respect to the specular reflectance both the aluminum on ground glass and nickel surfaces give similar results as shown in Fig. 5. This indicates, as is shown in Fig. 2, that the roughness characteristics of the two materials are similar.

Considering all of the above facts, the difference between the absolute hemispherical–angular reflectances of nickel and other surfaces is thought to be associated with high surface stresses caused particularly by changes in the crystalline structure of the nickel [6]. These changes could result from the grinding process, contamination of the surface, by the grinding compounds (inclusion of grinding grit into the surface) and by the sputtering process used to apply the thin film in the case of ground glass substrate. The situation of highly stressed thin films of nickel on glass substrates has been observed in work on microminiature electronic circuits [6]. This causes large variations in the optical properties of the surfaces. Similar effects were found for various types of surface preparations of nickel on smooth surfaces [7] and for roughened surfaces [8].

According to Davies [5], the angular–hemispherical reflectance of a roughened surface to a perfectly smooth surface for $\sigma_o/\lambda > 1{\cdot}0$ is

$$\frac{\rho_{ah}}{\rho_{ah,p}} = \frac{1}{32\pi^2 \cos\psi}\left[\frac{a}{\sigma_o}\right]^2 \int_0^{\pi/2}\int_0^{2\pi} [(\cos\theta + \cos\psi)]\, e^{-z} (\sin\theta \, d\theta \, d\varphi)$$

$$z = \tfrac{1}{2}\left(\frac{a}{\sigma_o}\right)^2 \left[\frac{(\sin\theta\cos\varphi - \sin\psi)^2 + \sin^2\theta\sin^2\varphi}{(\cos\theta + \cos\psi)^2}\right]. \qquad (1)$$

Three curves calculated using values of a^2/σ_o^2 of 10, 15 and 20 are shown in Fig. 2 for the distribution function of reflected radiation, and a value of 15 best describes the experimental results. Using the relation between the specular reflectance and bi-angular reflectance of a scattering surface in the specular direction [4], the ratio of the specular reflectance of a scattering surface to the specular reflectance of a polished surface becomes

$$\frac{\rho_s(\psi)}{\rho_{s,p}(\psi)} = \frac{1}{8\pi^2}\frac{a^2}{\sigma_o^2}\cos\psi\,\Delta\omega_i \qquad (2)$$

Since $\rho_{ah,p}(\psi) \equiv \rho_{s,p}(\psi)$, the ratio of reflectances given by equation (1) can be normalized by equation (2) to yield ρ_{ah}/ρ_s. Using a^2/σ_o^2 of 10, 15 and 20, calculations of ρ_{ah}/ρ_s are shown in Fig. 5. Again the value of $a^2/\sigma_o^2 = 15$ agrees most closely with the experimental results. Finally, equation (2) is used to calculate the specular ray reflectance of the scattering surface for the various values of a^2/σ_o^2 and one finds that the results are not in agreement with the experiment. For nickel the experimental value is approximately 0·001, and for aluminum it is between 0·002 and 0·003. If agreement with the aluminum data is the desired result, for the case, $a^2/\sigma_o^2 = 15$, it appears that Davies' equation must be multiplied by a factor of four. The specular ray reflectances are in agreement with the aluminum results when the correction is applied.

It should be pointed out that Davies' equation (1) can be conservatively used at most for angles of incident ψ up to 20°. The results of Torrance and Sparrow [9] are useful here in making this assessment. It has been suggested that equation (1) is in error [10] and strongly depends on a^2/σ_o^2 and ψ. The strong dependency on a^2/σ_o^2 is illustrated in Fig. 5. The disagreement of experimental data and equation (1) [10] was in the back-scattering azimuth ($\varphi = 180°$).

Before any complete assessment for small angles of incident can be made of equation (1), more precise data are required, specifically of the type reported in [9].

A word of caution about using equation (1) for very small values of wavelength compared to surface roughness. Porteus [11] has demon-normalized results. This technique thus gives a the RMS slope M, and the autocovariance length a for describing the reflectance under these conditions.

The preceding discussion has been centered around surfaces of isotropic roughnesses. Russell [3] presents angular–hemispherical reflectances for surfaces with unidirectional roughness prepared by sanding the surface in one direction with various grades of emery paper. Samples of pure copper and of stainless steel were prepared.

The results of [3] are normalized according to the procedure presented in this paper, and the mean roughness height, measured by a profilometer, is used in the roughness ratio. The final result is shown in Fig. 6, and the trend of undirectional roughness is similar to the isotropic the RMS surface roughness to incident wavelength. This treatment yields a single curve for aluminum, gold, copper and stainless steel. The unidirectional roughness of the copper and stainless steel samples do not influence the

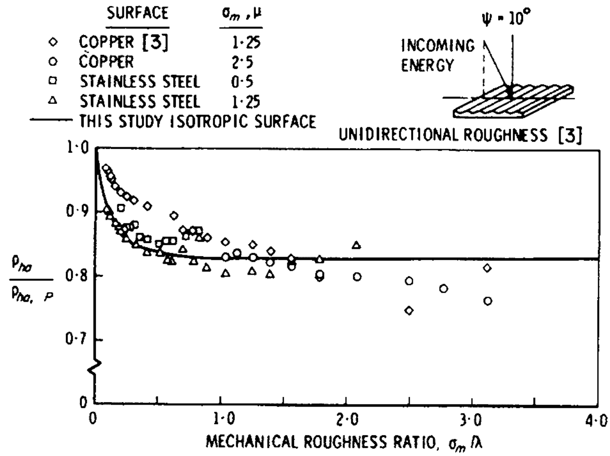

FIG. 6. Unidirectional surface roughness effects.

results. The results of [3] for copper between the wavelengths of 0·5–0·7 μ have not been included because over this wavelength range the reflectance changes from approximately 40–90 per cent, and it is difficult to obtain good results where the reflectance changes rapidly with wavelength.

CONCLUSIONS

Results of measurements of hemispherical reflectance characteristics of roughened surfaces are presented for aluminum, gold, platinum, and nickel films on substrate materials of glass and pure nickel. Various uniform surface roughnesses were obtained by standard optical grinding techniques.

A single curve may be obtained showing the effects of surface roughness on the monochromatic hemispherical reflectance. This is accomplished by plotting the ratio of the hemispherical reflectance of a roughened surface to that of a perfectly smooth surface vs. the ratio of possible means of intercomparing reflectance measurements of samples which have been roughened by several different methods. The nickel data do not agree with this general curve, and it is believed that surface effects such as lattice strain, etc., are the cause of this deviation.

The relationship between surface roughness and the wavelength of the incident radiation is quite evident. The data indicate that when the wavelength is less than the surface roughness, $\sigma_0/\lambda > 1$, the normalized reflectance is essentially a constant value. Previously it was assumed that the reflectance would decrease as a smooth function of σ_0/λ. Also as the wavelength becomes larger than the surface roughness, the reflectance approaches that of the smooth surface. These results were observed for the four films tested on both substrate materials.

ACKNOWLEDGEMENTS

The results of research presented were obtained by ARO, Inc. (a subsidiary of Sverdrup and Parcel, Inc.), contract operator of the AEDC under Contract AF40(600)-1200. The work was conducted under ARO Project Number SW2407, and was carried out by the Aerospace Environmental Facility of the ARO, Inc.

The authors wish to acknowledge the Heat Transfer Laboratory, Department of Mechanical Engineering, University of Minnesota for their contribution to this report by supplying some of the test surfaces.

REFERENCES

1. H. E. BENNETT and J. O. PORTEUS, Relation between surface roughness and specular reflectance at normal incidence, *J. Opt. Soc. Am.* **51**, 123 (1961).
2. R. C. BIRKEBAK and E. R. G. ECKERT, Effects of roughness of metal surfaces on angular distribution of monochromatic reflected radiation, *J. Heat Transfer* **87C**, 85 (1965).
3. D. A. RUSSELL. The spectral reflectance of rough surfaces in the infrared, Master Thesis, University of California, Berkeley, 1961.
4. K. E. TORRANCE and E. M. SPARROW, Biangular reflectance of an electric nonconductor as a function of wavelength and surface roughness, *J. Heat Transfer* **87C**, 283 (1965).
5. H. DAVIES, The reflection of electromagnetic waves from a rough surface, *Proc. Inst. Elect. Engrs* **101**, 209 (1954).
6. R. BELSER, Experimental Station, Georgia Institute of Technology, Private communication.
7. J. R. BEATTIE and G. K. T. CONN, Optical constants of metals in the infra-red—conductivity of silver, copper and nickel, *Phil. Mag.* **46**, 989 (1955).
8. R. E. ROLLING, A. I. FUNAI and J. R. GRAMMER, Investigation of the effect of surface condition on the radiant properties of metals, Air Force Systems Command, Wright–Patterson Air Force Base, Ohio, TR No. AFML-TR-64-363 (1964).
9. K. E. TORRANCE and E. M. SPARROW, Off-specular peaks in the directional distribution of reflected thermal radiation, *J. Heat Transfer* **88C**, 223 (1966).
10. L. M. HEROLD and D. K. EDWARDS, Bidirectional reflectance characteristics of rough, sintered-metal, and wire-screen surface systems, *AIAA Jl* **4**, 1802 (1966).
11. J. O. PORTEUS, Relation between the height distribution of a rough surface and the reflectance at normal incidence, *J. Opt. Soc. Am.* **53**, 1394 (1963).

Résumé—On a mesuré le pouvoir réflecteur total de surfaces métalliques avec une rugosité uniforme et contrôlée en employant une sphère en soufre intégratrice en rayonnement infrarouge et un spectromètre Beckman DK-2A. Les surfaces étudiées étaient du verre dépoli et du nickel recouvert de films d'aluminium, d'or, de platine et de nickel. Les résultats indiquent qu'au delà d'un rapport de la rugosité de surface à la longueur d'onde incidente $\sigma_0/\lambda \cong \lambda$, les valeurs normalisées pour l'aluminium, l'or et le platine peuvent être représentées par une courbe unique. Ceci était vrai pour les deux cas d'une rugosité uniforme unidirectionnelle et d'une rugosité uniforme, bien que les résultats pour le nickel dévient de cette courbe. On croit que les causes pour cette déviation sont liées aux contraintes de surface produites par des changements de structure cristalline et on les discute ici.

Zusammenfassung—Messungen der hemisphärischen Reflexion von metallischen Oberflächen mit bestimmter einheitlicher Oberflächenrauhigkeit wurden mit Hilfe einer infraroten, integrierenden Schwefelkugel und einem Beckmann DK-2A Spektrometer durchgeführt. Die untersuchten Oberflächen bestanden aus Milchglas und Nickel, beschichtet mit Aluminium, Gold, Platin, sowie aus reinem Nickel. Die Ergebnisse zeigen, dass ab einem Verhältnis Oberflächenrauhigkeit zu Wellenlänge der einfallenden Strahlung $\sigma_0/\lambda = 1$, die normalisierten Werte für Aluminium, Gold und Platin durch eine einzige Kurve wiedergegeben werden können. Dies gilt sowohl für einheitlich gleichgerichtete als auch für isotrope Rauhigkeiten, obwohl die Nickelwerte von dieser Kurve abweichen. Als Grund dieser Abweichungen werden Oberflächenspannungen angenommen, die von Veränderungen in der kristallinen Struktur herrühren. Sie werden in der Arbeit diskutiert.

Аннотация—Измерения полусферической отражательной способности металлических поверхностей, имеющих контролирующую однородную шероховатость, были сделаны, используя инфракрасный интегрирующий шар из серы и спектрометр Бекмана ДК-2А.

Рассматриваемые поверхности были изготовлены из стекла и никела и покрыты пленками алюминия, золота, платины и никеля. Данные показывают, что кроме отношения шероховатости поверхности к падающей длине волны, $\sigma_0/\lambda \cong 1$, нормализованные данные для алюминия, золота и платины могут быть представлены одной кривой. Это справедливо как для однородной ненаправленной шероховатости, так и для изотропной шероховатости, хотя данные для никеля отклоняются от этой кривой. Причины этого отклонения, вероятно, связаны с поверхностными напряжениями, вызванными измерениями в кристаллической структуре, и они обсуждаются в этом докладе.